Citar como:
F.D. Bianchi, R.S. Sánchez-Peña, Garelli F., Online adjustable LPV controller for artificial pancreas systems, Biomedical Signal Processing and Control, Vol. 86, 2023.
DOI: 10.1016/j.bspc.2023.105164

Online adjustable linear parameter-varying controller for artificial pancreas systems

Fernando D. Bianchi[a,c,*], Ricardo S. Sánchez-Peña[a,c], Fabricio Garelli[b,c]

[a] *Instituto Tecnológico de Buenos Aires (ITBA), Argentina*
[b] *Universidad Nacional de La Plata (UNLP), Buenos Aires, Argentina*
[c] *CONICET, Argentina*

Abstract

The purpose of this article is to present a non-hybrid controller for the Artificial Pancreas (AP) problem focused on long-term clinical trials and home-use applications. It includes physical activity and unannounced meals. The controller is based on a robust gain-scheduled algorithm with a Linear Parameter-Varying (LPV) structure. It accounts for the time-varying dynamics of the problem by adapting in real-time according to measured glucose levels, and allows online fine-tuning during tests and periodic evaluations without the need of controller redesign. The proposed fully parameterized LPV control adds several features to our previous results, accounts for the main perturbations of the AP problem and simplifies its implementation. In-silico tests show that the achieved performance is similar or better than our previous Automatic Regulation of Glucose (ARG) algorithm, tested in two clinical trials, with the addition of the features mentioned before.

Keywords: Artificial pancreas, Diabetes type 1, LPV control, insulin-on-board,

1. Introduction

The Artificial Pancreas (AP) problem has been given considerable importance in the last decades as a means of improving the quality of life of Type 1 Diabetes Mellitus (T1DM) patients. A reference of several world-wide groups working in this problem that have performed clinical trials can be found in [24]. Several results have been reported in this area which involve detection of meals [21, 31, 14], meals and physical activity (PA) [2], closed-loop algorithms with unannounced meals [16, 25, 28, 10, 3] and tested in clinical trials [5, 10, 18, 19]. In general, the time-varying dynamics are not accounted for in the design. More importantly, these methodologies require a re-design of the controller if changes are produced during the clinical test.

The group in Argentina, from UNLP and ITBA, has focused on patient's autonomy, i.e. non-hybrid algorithms which require the least intervention of the patient, unannounced meals and possibly PA. It has performed three previous clinical trials, the only ones in Latin America. The first one tested 5 patients during 36 hours in the Hospital Italiano of Buenos Aires in November 2016 with a platform (DiAs) and an algorithm from the University of Virginia. In June 2017 a similar test was performed [23, 29] but with a control algorithm developed locally. The third trial was ambulatory (out-patient) and lasted 6 days with 5

*Corresponding author.
Email addresses: fernando.bianchi@ib.edu.ar (Fernando D. Bianchi), rsanchez@itba.edu.ar (Ricardo S. Sánchez-Peña), fabricio@ing.unlp.edu.ar (Fabricio Garelli)

patients during march 2021 [12]. In the last two trials, the ARG control algorithm was used [7] in conjunction with a safety layer to minimize hypoglycemia [22], and proved to work properly with unannounced meals [11]. In the last clinical test, a monitoring platform developed by the UNLP, named InsuMate was used [13].

The ARG controller is based on a control-oriented model developed by members of this group [8] which has been used to design a switched LQG controller [7], and combined with the SAFE [22] procedure to prevent hypoglycemia. This control-oriented model is tuned to each patient by means of his/her Total Daily Insulin (TDI). The ARG algorithm provided good results in our last two clinical trials, but certain shortcomings need to be solved.

First, although based on a Linear Parameter-Varying (LPV) control-oriented model, the controller was designed as a switched LQG control in order to simplify the programming in both, the DiAs and InsuMate platforms. Therefore, this lacks the continuous time-varying capacity of an LPV control.

Second, during the clinical trials it was observed that, due to changes in the insulin sensitivity and other parameters as the clinical TDI, a real-time redesign of the controller had to be made to increase performance. In the case of the ARG, many off-line computations had to be achieved for this purpose, e.g. tuning of the model to the new TDI, computation of the LQG matrices, model reduction, etc. Hence, a controller that could be adjusted online according to the patient's behavior during the test without the need of a re-design, would be highly convenient. This is particularly important in our future phase-4 trial with patients at home and during a long period of time.

Third, it is important not only to take into account the meals, but also PA as perturbations to the patient's regulation. Recently we have designed a switched LPV controller which meets those needs [6].

In this article, a new algorithm based on LPV control tools is developed so that it can be tuned during the trials without the need for a controller redesign and also takes into account unannounced meals and PA. Two additional parameters are added in order to finely adjust the controller to the particular patient based on information obtained during the clinical trials. A new measure based on variables commonly used by physicians is also introduced in order to help in the tuning of these parameters. This novel controller parameterization aims to find the most suitable trade-off between good glucose regulation and low hypoglycaemia risk for each patient.

This work is organized as follows. Section 2 describes previous results by the authors and Section 3 the new LPV control scheme suitable for *in-situ* tuning. Section 4 presents the main results and the paper ends with some concluding remarks in Section 5.

2. Previous results

The initial version of the ARG algorithm was based on switched LQG controllers combined with the SAFE layer. An updated version, which contemplates also PA and based on a purely LPV framework has been presented in [6]. Figure 1 sketches the AP strategy of the latter algorithm. The core of this strategy is the switched LPV controller and the SAFE algorithm. The former consists of two LPV controllers: $K_1(\rho)$ more conservative and $K_2(\rho)$ more aggressive for situations with high glucose increase rates. Both controllers are parameterized by a function of the glucose g and switched depending on the controller mode signal. The SAFE module is basically a safety layer that limits the insulin command produced by the LPV controller according to the Insulin On Board (IOB) in order to minimize risk of hypoglycemia imposing an upper limit $\overline{\mathrm{IOB}}$.

The core system receives two signals besides the glucose measure fed-back by the CGM system. These additional signals are generated by the Mode Selector according to the patient heart rate (HR), an exercise announcement manually set by the patient and the hyperglycemia detection signal. With these inputs, the

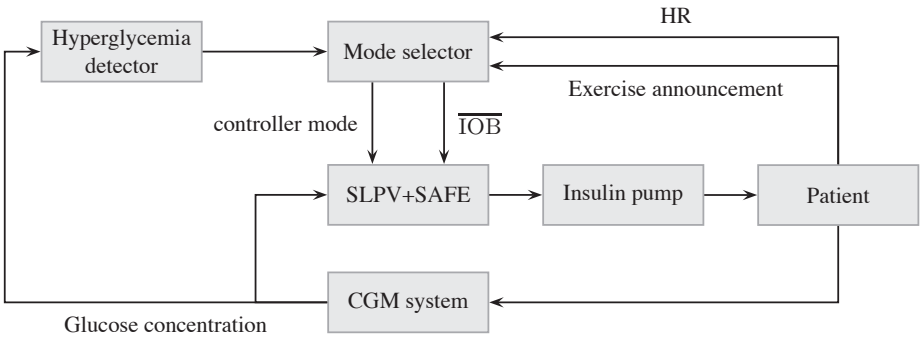

Figure 1: Diagram of the AP strategy proposed in [6].

Mode Selector produces two commands for the switched LPV controller and the SAFE module according to four operation modes:

1. *Conservative mode:* when the glucose is close to the basal level, the conservative LPV controller K_1 handles the glucose regulation and the SAFE module operates with a limit $\overline{\mathrm{IOB}} = \overline{\mathrm{IOB}}_{\mathrm{s}} = \mathrm{IOB}_{\mathrm{b}} + 40$ g/CR, where $\mathrm{IOB}_{\mathrm{b}}$ is the estimated IOB value at basal input rate and CR is the patient dependent insulin-to-carbohydrate ratio in U/g.
2. *Aggressive mode:* is applied when the hyperglycemia detector determines a fast increase in the glucose value. In this mode, the aggressive LPV controller K_2 regulates the glucose and the SAFE module works with the limit $\overline{\mathrm{IOB}} = \overline{\mathrm{IOB}}_{\mathrm{m}} = \mathrm{IOB}_{\mathrm{b}} + 55$ g/CR.
3. *Exercise mode:* is triggered a certain instant before the exercise start time manually indicated by the patient and is maintained for at least 60 minutes. In this mode, the conservative LPV controller K_1 regulates the glucose and the $\overline{\mathrm{IOB}}$ used by the SAFE module is set depending on the surface shown in Figure 2.
4. *Post-exercise mode:* is set during 8 hours after the exercise in order to minimize the risk of hypoglycemia and consists in setting $\overline{\mathrm{IOB}} = \overline{\mathrm{IOB}}_{\mathrm{s}}$ whereas the LPV controller is selected according to the signal sent by the Hyperglycemia Detector.

The purpose of the present article is to fully parameterize this control strategy as a function of easily determined patient characteristics and thus to be able to adjust the control strategy to the patient without specific modelings and designs. As observed from the previous description, the only part that must be designed for a specific patient is the LPV controller, performed previous to a clinical trial. Hence a new design approach is proposed in the next section. In order to keep the control strategy simple, the switching is eliminated and only one LPV controller is designed. Thus in the new AP strategy the Mode Selector from Figure 1 only produces the signal $\overline{\mathrm{IOB}}$.

3. Fully parameterized LPV control methodology

The patient's glucose response to an insulin bolus exhibits significant changes among subjects. On the other hand, the preservation of the patient's comfort and safety also limits the tests that can be performed to identify accurate mathematical descriptions. This makes quite difficult to design high performance and patient-tuned model-based controllers. Therefore, the aim of the proposed strategy presented here is to design a fully parameterized LPV controller that can be adjusted *in-situ* for any particular patient during the

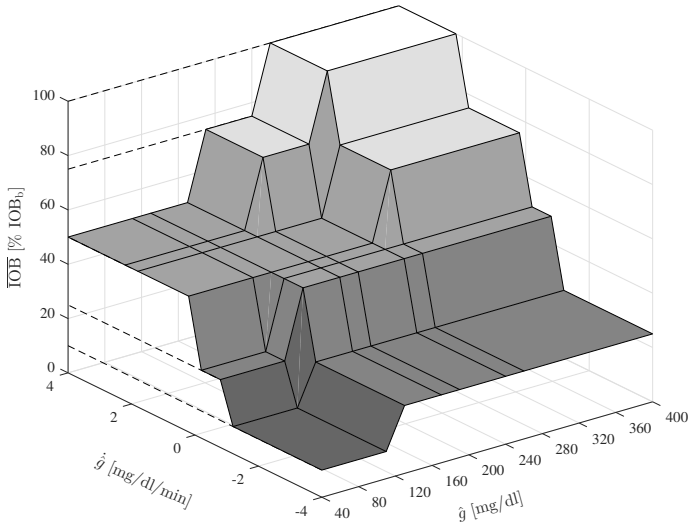

Figure 2: $\overline{\mathrm{IOB}}$ surface as a function of g and $\dot{g}$. The $\overline{\mathrm{IOB}}$ is expressed as percentage of $\mathrm{IOB_b}$ [6].

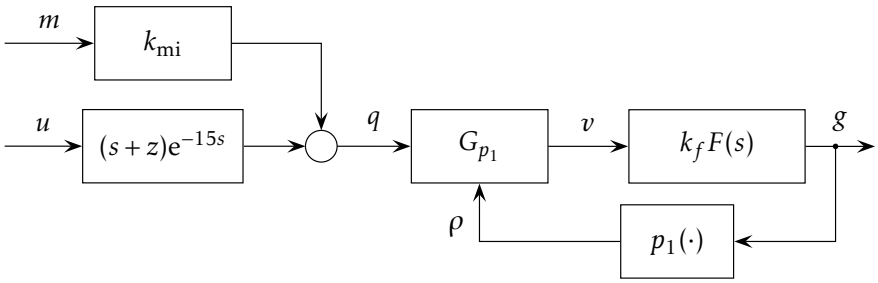

Figure 3: LPV representation of the mapping meal/insulin-glucose

device configuration and subsequent adjustments throughout the clinical trial, without the need to redesign the controller. This is clearly applicable to a clinical trial situation.

For this purpose, the control-oriented model inspired by [8] and sketched in Figure 3 is used for the controller design, where m is the meal, u the insulin and g the glucose. The filter $F(s)$ is given by

$$F(s) = \frac{b_0}{s^2 + a_1 s + a_0}. \tag{1}$$

This filter, the zero z and the gain k_{mi} are assumed common for all patients and their parameters can be obtained as indicated in [8]. Based on results obtained from the distribution version of the UVA simulator, the following values were obtained: $a_0 = 0.0129$, $a_1 = 0.017$, $b_0 = 7.1010 \times 10^{-4}$, $z = 0.1501$, $k_{\mathrm{mi}} = -0.041$. The 15 minute delay is approximated as

$$G_d(s) = \mathrm{e}^{-15s} \approx \frac{0.008}{(s+0.2)^3}. \tag{2}$$

The operator G_{p_1} represents the LPV system

$$G_{p_1}(\rho) : \begin{cases} \dot{x}_p = -\rho x_p + q, \\ v = x_p, \end{cases} \tag{3}$$

where the parameter $\rho = p_1(g)$ is a piecewise polynomial depending on the glucose g, which models the bandwidth changes observed in the response at different glucose concentrations [8].

The gain k_f models the inter-patient variability and is determined using the 1800/TDI rule as shown in [8]. For each patient in the UVA simulator, a gain k_f is computed such that the control-oriented model exhibits the glucose drop given by 1800/TDI. Fitting a first order polynomial to these points, the following expression can be used to adjust the model for a particular patient

$$k_f(\theta_1) = c_{TDI,1}\,\theta_1 + c_{TDI,0}, \tag{4}$$

where θ_1 is the patient TDI, and $c_{TDI,0} = 2.3327$ and $c_{TDI,1} = -0.0228$ are constant coefficients.

Assuming that:

$$F(s) : \begin{cases} \dot{x}_f = A_f x_f + B_f v, \\ g = C_f x_f \end{cases} \tag{5}$$

$$(s+z)G_d(s) : \begin{cases} \dot{x}_d = A_d x_d + B_d u, \\ q_1 = C_d x_d \end{cases} \tag{6}$$

the entire model can be expressed as

$$G(\rho, \theta_1) : \begin{cases} \dot{x} = A(\rho)x + B_m m + B_u u, \\ g = C(\theta_1)x, \end{cases} \tag{7}$$

where $x = [x_d^T \; x_p \; x_f^T]^T$, being $x_d \in \mathbb{R}^3$, $x_p \in \mathbb{R}$, $x_f \in \mathbb{R}^2$,

$$\begin{aligned} A(\rho) &= \begin{bmatrix} A_d & 0 & 0 \\ C_d & -\rho & 0 \\ 0 & B_f & A_f \end{bmatrix}, \quad B_m = \begin{bmatrix} 0 \\ k_{\text{mi}} \\ 0 \end{bmatrix}, \quad B_u = \begin{bmatrix} B_d \\ 0 \\ 0 \end{bmatrix}, \\ C(\theta_1) &= \begin{bmatrix} 0 & 0 & k_f(\theta_1) C_f \end{bmatrix}. \end{aligned} \tag{8}$$

The parameter set is defined as

$$\mathcal{P} = \{p_{1,\min} \leq \rho \leq p_{1,\max}\} \times \{\text{TDI}_{\min} \leq \theta_1 \leq \text{TDI}_{\max}\}, \tag{9}$$

with $p_{1,\min} = 0.0028$ and $p_{1,\max} = 0,013$ from [8], $\text{TDI}_{\min} = 34$ U and $\text{TDI}_{\max} = 72$ U, considering the 11 patients in the UVA/Padova simulator. To sum up, the dynamic mapping meal/insulin-glucose is described by an LPV model of order 6 and two parameters (ρ, θ_1) taking values in the set $\mathcal{P}$.

The previous LPV description is used in the closed-loop setup illustrated in Figure 4 in order to state the LPV controller design as the following multi-objective problem:

$$\begin{aligned} \min_{\tilde{K} \in \mathcal{K}(\rho,\theta_1,\theta_2)} \quad & ||T_1||_2, \\ \text{subject to} \quad & ||T_2||_{\mathcal{L}_2} \leq 1, \end{aligned} \tag{10}$$

where $\mathcal{K}(\rho, \theta_1, \theta_2)$ is the set of stabilizing LPV controllers, T_1 denotes the mapping from m to $\tilde{e}$, T_2 the mapping from r to $\tilde{u}$. The symbol $||\cdot||_2$ denotes the generalized H_2 norm, and $||\cdot||_{\mathcal{L}_2}$ the $\mathcal{L}_2$ induced norm. This multi-objective design aims at minimizing the maximum deviations of the glucose g from the basal value when a meal (assumed as pulses of carbohydrates) is ingested. Whereas, the control action (insulin) is bounded and a certain degree of robustness against un-modeled dynamics is ensured.

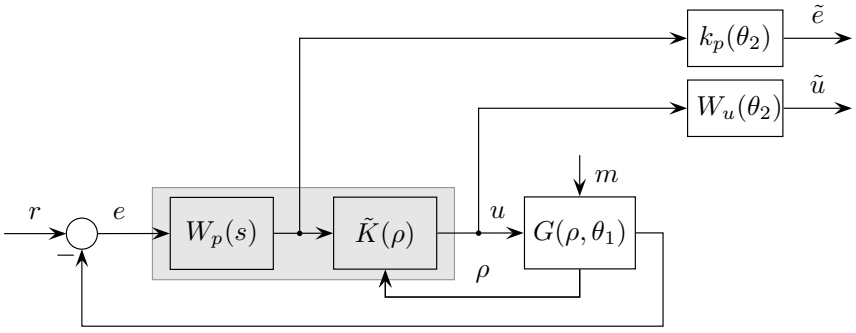

Figure 4: Closed-loop setup used for the controller design

The weighting functions in the setup shown in Figure 4 are taken as

$$W_u(s, \theta_2) = (k_{u,0} + (1 - \theta_2)k_{u,1}) \frac{s + 0.1}{s + 10}, \tag{11}$$

$$W_p(s) = \frac{1}{100s + 1}, \tag{12}$$

$$k_p(\theta_2) = k_{p,0} + \theta_2 k_{p,1}, \tag{13}$$

where $k_{u,0} = 5$, $k_{u,1} = -4.5$, $k_{p,0} = 10$, and $k_{p,1} = 490$. The parameter θ_2 ranges between 0 and 1. Higher values of θ_2 penalize more the glucose error and less the control action. Therefore, the parameter θ_2 will determine the aggressiveness of the resulting controller.

The plant augmented with the weighting functions (11)-(13) is an LPV system of order 8 with three parameters: ρ, θ_1, θ_2. The resulting controller

$$K(\rho, \theta_1, \theta_2) = W_p(s)\tilde{K}(\rho, \theta_1, \theta_2) \tag{14}$$

depends on two types of parameters varying at different time-scales[1]. Parameter ρ is employed to adapt the controller in real-time according to the current value of the glucose measurement at each time step, as a typical gain-scheduled LPV controller. On the other hand, parameters θ_1 and θ_2 tune the controller in order to adjust it to the patient's TDI and the desired controller aggressiveness. This tuning can be seen as if parameter θ_1 selects the nominal model and θ_2 the model uncertainty bound. These two parameters are set during periodic device configurations, observing the closed-loop patient's response, but they do not change during the normal controller operation. They are used to finely tune *in-situ* for each patient, without the need of controller redesigns.

The optimization problem (10) can be efficiently solved with the algorithm introduced in [1] and implemented with Yalmip [15] and SeDuMi [27]. This algorithm relies on matrix Lyapunov functions that, together with the specifications given by the operators T_1 and T_2, defines the set of stabilizing controllers $\mathcal{K}$. In particular, parameter dependent Lyapunov functions permits us to consider the expected parameter variation rates and thus improves the controller performance. This can be employed to take into account the different time-scales of the two types of parameters during the controller design. The parameter ρ is expected to change at each sampling time (5 minutes) but the other parameters may remain constant during

[1]This factorization is necessary to ease the controller design, see [1] for more details.

days, until a new manual controller tuning is done. In the framework proposed in [1], this can be considered using the following parameter dependent Lyapunov functions

$$\begin{aligned} X(\theta_1,\theta_2) &= X_0 + \theta_1 X_1 + \theta_2 X_2, \quad \dot{X}(\theta_1,\theta_2) = 0, \\ Y(\theta_1,\theta_2) &= Y_0 + \theta_1 Y_1 + \theta_2 Y_2, \quad \dot{Y}(\theta_1,\theta_2) = 0. \end{aligned} \tag{15}$$

By imposing zero time derivatives of these functions, the design procedure takes into account that the parameters θ_1 and θ_2 will not change[2]. The absence of the parameter ρ in these expressions indicates that this parameter will vary frequently during the controller operation. This consideration helps to improve the controller performance as it allows us to indicate that θ_1 and θ_2 will be almost constant compared with the changes of ρ.

The differential equation to compute the control action at each step-time can be expressed as

$$K(\rho): \begin{cases} \dot{x}_c = (A_{c,0} + \rho\, A_{c,1})\, x_c + (B_{c,0} + \rho\, B_{c,1})\, e, \\ u = (C_{c,0} + \rho\, C_{c,1})\, x_c + (D_{c,0} + \rho\, D_{c,1})\, e, \end{cases} \tag{16}$$

where the matrices $A_{c,0}, \ldots, D_{c,1}$ are obtained after assigning the particular values of θ_1 and θ_2 in the controller matrices. Notice that once the parameters θ_1 and θ_2 are set during the fine-tuning stage, the controller only depends on the parameter ρ similarly to the strategy presented in [8]. More details about the controller expressions and design can be found in Appendix A.

4. Results

The aim of the methodology proposed in the previous section is to produce a controller adjustable to each patient without extensive tests and complex redesigns, adequate for a clinical trial environment. The adjustments for the *in-situ* tuning to each patient will be performed by θ_1 and θ_2. The first will be modified according to (4) when the patient's TDI significantly moves during the test with respect to its clinical value. The second one graduates the aggressiveness of the controller according to the hyper- and hypoglycemias of the patient during the trial. As explained before, a single LPV controller designed off-line allows changes in both parameters during the trial.

In order to evaluate the strategy a representative simulation scenario was analyzed using the distribution version of the UVA/Padova simulator. The scenario is similar to the one presented in [6]. The patient ingests three meals:

- 40 g meal at 7 AM,
- 70 g meal at 12 PM, and
- 60 g meal at 7 PM.

At 4 PM, the patient does a 30 min bout of moderate exercise, which is announced to the controller 30 minutes before starting. Here, as considered in [6], intra-patient variations have been treated as uncertainty, which can be taken into account by an adequate selection of weight W_u [4]. Another alternative, not considered here, would be to add an extra parameter to the LPV controller, which should measure or estimate these variations in real time [17]. In the simulations, the LPV controller and the remaining elements in

[2] Actually it will have very few changes during a complete clinical test.

Figure 1 were discretized at each sampling time of 5 minutes. In order to obtain realistic results, the insulin pump quantification errors were also included. The measurement noise was not considered to ease the comparison of the responses.

Figure 5 shows the glucose and the insulin injected by the pump in case of Patient 11 (average patient). The thick, black line corresponds to the response when an LPV controller is designed for a model tuned for the particular patient. That is, the gain k_f is determined from the open-loop patient response to 1 U insulin bolus as indicated in [8] and not using the approximation (4). As this would be the ideal situation, it is used as the baseline for comparisons. This controller is designed with the same closed-loop setup in Figure 4 and the weighting functions (11)-(12), with $k_u = 2.75$ and $k_p = 255$. The remaining lines are the closed-loop evolution obtained with the proposed controller using a grid of 11 values for the parameter θ_2 between 0 (more conservative) and 1 (more aggressive). The gray areas indicate the instant in which carbohydrates are ingested, whereas the green area marks the period of PA. As mentioned before, besides the scheduling variable $\rho = p_1(g)$, the resulting LPV controller has two parameters to be tuned *in-situ*: the gain $k_f(\theta_1)$ and the aggressiveness θ_2. The first one is set according to the expression (4) with the patient's TDI, 40 U in the case of Patient 11. The numbers in the legend corresponds to the values of θ_2. Clearly, the most aggressive controller ($\theta_2 = 1$) reduces the glucose peak but at the expense of a larger drop, which approaches hypoglycemia. On the other side, the most conservative setting ($\theta_2 = 0$) yields a higher initial glucose peak but the drop is less marked, with a lower risk of hypoglycemia. These results demonstrate that the proposed controller parameterization enables us to achieve a similar response to the one obtained with the baseline controller.

The parameter θ_2 allows us to set the aggressiveness of the controller according to the insulin sensitivity of the particular patient. The aim is to achieve a trade-off between a fast glucose regulation to avoid hyperglycaemia and a low risk of hypo-glycaemia. As a guide to select this parameter, the following measure, based on the well-known LBGI and HBGI indices, can be used:

$$m_{\ell h}(B_{\ell i}, B_{hi}) = \begin{cases} 1, & \text{if LBGI} \geq B_{\ell i} \text{ or HBGI} \geq B_{hi} \\ w_\ell \cdot \text{LBGI} + w_h \cdot \text{HBGI}, & \text{otherwise,} \end{cases} \tag{17}$$

where the upper bounds are $B_{\ell i} = 2.5$ and $B_{hi} = 4.5$ [26, 30] for a diabetic patient. The weights w_ℓ and w_h are used to scale the differences between bounds, so that the parameter $m_{\ell h}$ does not increase above unity when $\text{LBGI} < B_{\ell i}$ and $\text{HBGI} < B_{hi}$, defined as the *safe region*. Therefore $w_\ell = 0.5/B_{\ell i}$ and $w_h = 0.5/B_{hi}$. The top plot in Figure 6 shows the LBGI and HBGI indices for the Patient 11 in the UVa/Padova simulator, for several values of θ_2. The measure $m_{\ell h}$ is shown in the bottom plot in Figure 6 with solid line and square markers. In this case, all values of θ_2 are safe, although values between 0.7 and 0.8 will produce lower values of $m_{\ell h}$. Notice that the index $m_{\ell h}$ depends on the bounds B_{li} and B_{hi}. Hence, to achieve lower values of LBGI-HBGI [30], these bounds can be set to $B_{\ell i} = 1.5$, $B_{hi} = 3$, e.g. for non-diabetic patients. In this case, the index $m_{\ell h}$ is restricted to a narrower region, as indicated in the bottom plot in Figure 6 with solid line and triangle markers. In both cases, it can be observed that there is a minimum suggesting the most suitable value for θ_2.

In Figure 7, the closed-loop response under the previously described scenario for 10 patients in the UVa/Padova simulator[3] is presented. The thick, black line corresponds to the median. The top plot shows the responses using the baseline control tuning, i.e. obtaining k_f from an open-loop experiment and using the weights (11)-(12), with $k_u = 2.75$ and $k_p = 255$, as mentioned before. The middle plot presents the closed-loop responses with the new controller using $\theta_2 = 0.5$. The bottom plot displays the responses

[3] Adult Patient 7 from the database has an insulin sensitivity that is not coherent with its TDI, hence, it has been excluded.

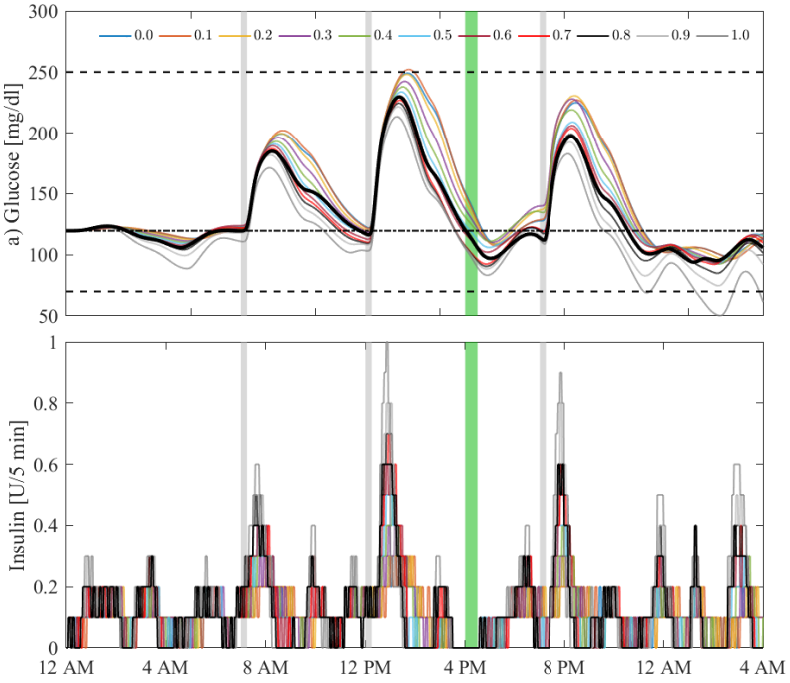

Figure 5: Nonlinear simulations of the closed-loop responses for the baseline controller (black line) and the proposed controller with several settings of the parameter θ_2. The gray areas indicate the meal ingestion period and the green area when physical activity is performed.

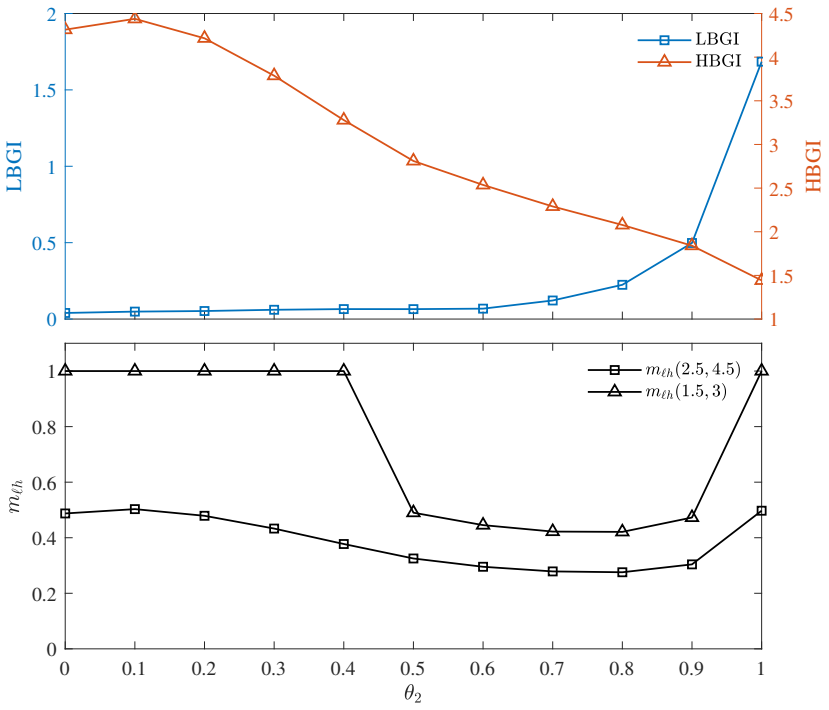

Figure 6: LBGI and HBGI indices and the measure $m_{\ell h}$ for the Patient 11 in UVa/Padova Simulator for several values of θ_2.

Table 1: Values of θ_2 used to obtain the closed-loop responses in Figure 7c

Patient	θ_2	Patient	θ_2
1	0.8	6	0.9
2	0.8	8	0.9
3	0.9	9	0.6
4	0.6	10	0.8
5	0.8	11	0.8

Table 2: Average closed-loop results for all *in silico* adults corresponding to Figure 7. LGBI: Low blood glucose index, HBGI: High blood glucose index, IQR: Interquantile range, [20].

	Baseline			**New Control** ($\theta_2 = 0.5$)			**New Control** (θ_2 **in Table 1**)		
Overall	**Mean**	**Median**	**IQR**	**Mean**	**Median**	**IQR**	**Mean**	**Median**	**IQR**
Average blood glucose (mg/dl)	133.36	130.46	10.85	137.51	135.87	6.69	133.32	131.38	5.55
Coefficient of variation (%)	24.00	25.00	7.00	25.00	25.00	5.00	24.00	24.00	6.00
% time $<$ 70 mg/dl	0.00	0.00	0.00	0.00	0.00	0.00	0.00	0.00	0.00
% time in $[70, 140]$ mg/dl	68.16	70.79	16.24	65.75	68.47	13.56	70.12	71.77	11.01
% time in $[70, 180]$ mg/dl	88.08	90.27	8.98	85.09	86.76	7.56	87.61	87.60	6.25
% time $>$ 180 mg/dl	11.92	9.73	8.98	14.91	13.24	7.56	12.39	12.40	6.25
LBGI	0.22	0.14	0.19	0.11	0.11	0.07	0.14	0.13	0.05
HBGI	2.50	2.16	1.10	2.89	2.59	1.03	2.42	2.21	0.57

when the new controller is tuned with a particular value of θ_2 selected to achieve a trade-off between maximum and minimum glucose values by minimizing the value of $m_{\ell h}(2.5, 4.5)$. These values are given in Table 1 and were taken from the grid of values used for Figure 5. Table 2 summarizes the average closed-loop results corresponding to the simulations in Figure 7 based on the time consensus outcome metrics for glucose controller's performances given in [9]. It can be seen that most of the metrics are similar in the three cases, although the new controller with parameter θ_2 tuned to each patient achieves values closer to the baseline.

The *in-situ* tuning of this parameter allows the improvement of the closed-loop response, and suggests a methodology to finely tune the controller for each patient:

1. Configure the controllers as $\theta_1 = \text{TDI}$ (initial clinical value) and $\theta_2 = 0.5$.
2. Record the patient's behaviour during the trial and compute the index $m_{\ell h}$. Based on the information previously gathered try small changes in θ_2 taking into account that an increase of θ_2 reduces the maximum glucose value after meals but also increases the risk of hypoglycemia. Record the glucose again and recompute $m_{\ell h}$, if the value is lower try to increase θ_2, otherwise decrease it. Repeat the procedure seeking the minimum value of $m_{\ell h}$.

Notice that there is no need to redesign the controller to make these changes. In addition, take into account that the modifications of these parameters take place very few times during a clinical trial, as opposed to parameter $\rho(g)$ that may change every 5 min, in accordance with the assumptions in Section 3. Finally, the parameter modifications are easy to implement by non-technical personnel, e.g. physicians.

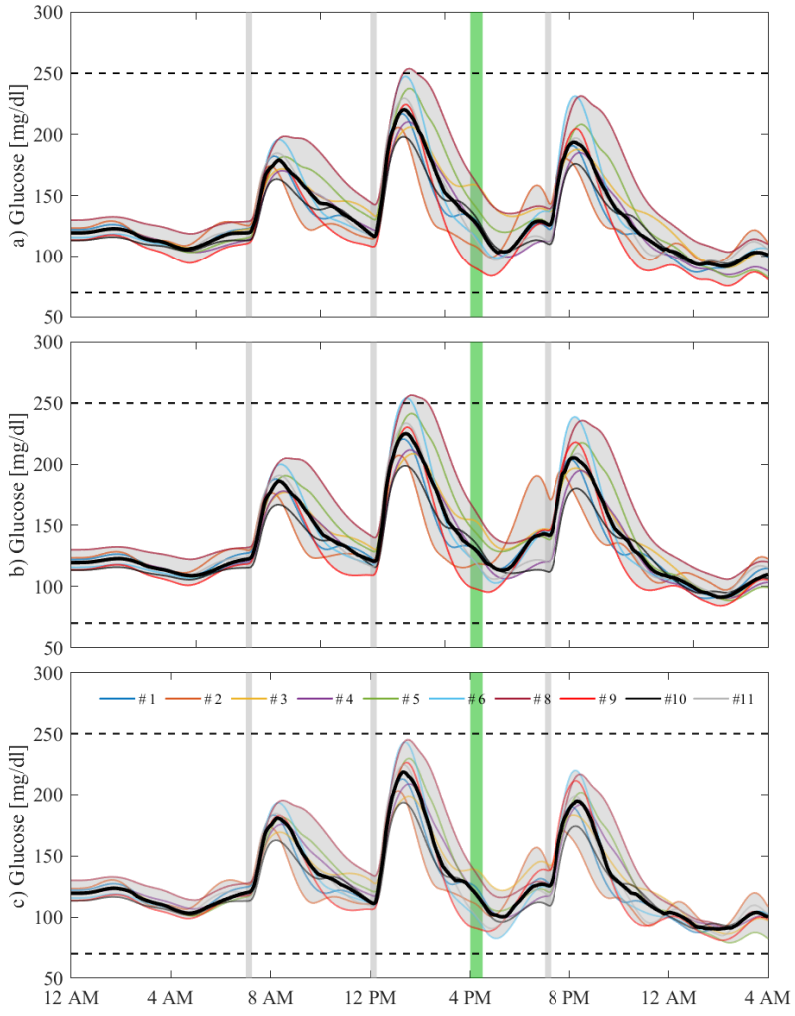

Figure 7: Nonlinear simulations of the closed-loop system for all patients in UVA simulator (except for subject 7) using several controllers. The gray areas indicate the meal ingestion period and the green area when PA is performed. a) Using the baseline control tuning, b) new controller with $\theta_2 = 0.5$, and c) new controller with θ_2 tuned to achieve a trade-off between maximum and minimum glucose peaks. The thick, black lines indicate the median response.

5. Conclusions

The high variability of the inter- and intra-patient glucose response makes it difficult to design high performance model-based AP. Therefore, a new LPV, fully parameterized controller has been proposed with the aim of improving the online tuning for any particular patient. This tuning can be made during the clinical trial by simply setting two parameters. The proposed AP scheme has been tested with the distribution UVa/Padova simulator under meal and PA disturbances. The results showed that the proposed parameterization is able to achieve similar performance to ideally tuned controllers.

Acknowledgments

The authors thank the financial support of ITBA, PIP-CONICET No. 2595, PICT No. 2554 and UNLP project I253.

Appendix A. LPV control design

For an augmented plant

$$\begin{aligned}
\dot{x} &= A(\rho,\theta_1,\theta_2)x + B_1(\rho,\theta_1,\theta_2)w + B_2 u,\\
z_1 &= C_1(\rho,\theta_1,\theta_2)x + D_{11}(\rho,\theta_1,\theta_2)w + D_{12}u,\\
z_2 &= C_2(\rho,\theta_1,\theta_2)x + D_{21}(\rho,\theta_1,\theta_2)w + D_{22}u,\\
y &= C_3 x + D_{31} w,
\end{aligned}$$

defining the mapping $T_1 : w \to z_1$ and $T_2 : w \to z_2$, the optimization problem (10) can be translated into solving a convex problem with the following LMI constraints:

$$\begin{bmatrix}
-\dot{\mathbf{Y}} + A\mathbf{Y} + B_2\hat{\mathbf{C}} + (\star) & \star & \star & \star \\
\hat{\mathbf{A}} + (A + B_2\hat{\mathbf{D}}C_3)^T & \dot{\mathbf{X}} + \mathbf{X}A + \hat{\mathbf{B}}C_3 + (\star) & \star & \star \\
(B_1 + B_2\hat{\mathbf{D}}D_{31})^T & (\mathbf{X}B_1 + \hat{\mathbf{B}}D_{31})^T & -I & \star \\
C_2\mathbf{Y} + D_{22}\hat{\mathbf{C}} & C_2 + D_{22}\hat{\mathbf{D}}C_2 & D_{21} + D_{22}\hat{\mathbf{D}}D_{21} & -I
\end{bmatrix} < 0,$$

$$\begin{bmatrix}
\mathbf{X} & \star & \star \\
I & \mathbf{Y} & \star \\
C_1\mathbf{Y} + D_{12}\hat{\mathbf{C}} & C_1 + D_{22}\hat{\mathbf{D}}C_3 & \mu I
\end{bmatrix} > 0,$$

$$D_{12} + D_{22}\hat{\mathbf{D}}D_{21} = 0,$$

with $\mu = \min \|T_1\|_2$ and

$$\hat{\mathbf{A}}(\rho,\theta_1,\theta_2) = \hat{\mathbf{A}}_0 + \hat{\mathbf{A}}_1\rho + \hat{\mathbf{A}}_2\theta_1 + \hat{\mathbf{A}}_3\theta_2, \tag{A.1}$$

$$\hat{\mathbf{B}}(\rho,\theta_1,\theta_2) = \hat{\mathbf{B}}_0 + \hat{\mathbf{B}}_1\rho + \hat{\mathbf{B}}_2\theta_1 + \hat{\mathbf{B}}_3\theta_2, \tag{A.2}$$

$$\hat{\mathbf{C}}(\rho,\theta_1,\theta_2) = \hat{\mathbf{C}}_0 + \hat{\mathbf{C}}_1\rho + \hat{\mathbf{C}}_2\theta_1 + \hat{\mathbf{C}}_3\theta_2, \tag{A.3}$$

$$\hat{\mathbf{D}}(\rho,\theta_1,\theta_2) = \hat{\mathbf{D}}_0 + \hat{\mathbf{D}}_1\rho + \hat{\mathbf{D}}_2\theta_1 + \hat{\mathbf{D}}_3\theta_2, \tag{A.4}$$

$$\mathbf{X}(\rho,\theta_1,\theta_2) = \mathbf{X}_0 + \mathbf{X}_1\theta_1 + \mathbf{X}_2\theta_2, \tag{A.5}$$

$$\mathbf{Y}(\rho,\theta_1,\theta_2) = \mathbf{Y}_0 + \mathbf{Y}_1\theta_1 + \mathbf{Y}_2\theta_2. \tag{A.6}$$

The constant matrices $\hat{\mathbf{A}}_0, \ldots, \mathbf{Y}_2$ of suitable dimensions are the decision variables to be found.

The parameters θ_1 and θ_2 are set during the AP configuration, as a result the functions (A.1)-(A.4) will depend only on ρ whereas the functions (A.5) and (A.6) will be constant matrices. Therefore, the parameter dependent matrices in (16) are obtained after substituting these matrices in the expressions:

$$A_c(\rho) = N^{-1}(\hat{\mathbf{A}}(\rho) - \mathbf{X}(A(\rho) - B_2\hat{\mathbf{D}}(\rho)C_2)\mathbf{Y} - \hat{\mathbf{B}}(\rho)C_2\mathbf{Y} - \mathbf{X}B_2\hat{\mathbf{C}}(\rho))M^{-T}, \tag{A.7}$$

$$B_c(\rho) = N^{-1}(\hat{\mathbf{B}}(\rho) - \mathbf{X}B_2\hat{\mathbf{D}}(\rho)), \tag{A.8}$$

$$C_c(\rho) = (\hat{\mathbf{C}}(\rho) - \hat{\mathbf{D}}(\rho)C_2\mathbf{Y})M^{-T}, \tag{A.9}$$

$$D_c(\rho) = \hat{\mathbf{D}}(\rho), \tag{A.10}$$

where M and N are selected to satisfy $I - \mathbf{XY} = NM^T$. The controller expressions (16) can be easily deduced from the previous equations. Further details can be found in [1].

References

[1] P. Apkarian and R.J. Adams. Advanced gain-scheduling techniques for uncertain systems. *IEEE Transactions on Control Systems Technology*, 6(1):21–32, 1998.

[2] Mohammad Reza Askari, Mudassir Rashid, Xiaoyu Sun, Mert Sevil, Andrew Shahidehpour, Keigo Kawaji, and Ali Cinar. Detection of meals and physical activity events from free-living data of people with diabetes. *Journal of Diabetes Science and Technology*, page 19322968221102183, 2022.

[3] Yazdan Batmani, Shadi Khodakaramzadeh, and Parham Moradi. Automatic artificial pancreas systems using an intelligent multiple-model PID strategy. *IEEE Journal of Biomedical and Health Informatics*, 26(4):1708–1717, 2021.

[4] F. D. Bianchi, M. Moscoso-Vásquez, P. Colmegna, and R. S. Sánchez-Peña. Invalidation and low-order model set for artificial pancreas robust control design. *Journal of Process Control*, 76:133 – 140, 2019.

[5] Torben Biester, Judith Nir, Kerstin Remus, et al. Dream5: An open-label, randomized, cross-over study to evaluate the safety and efficacy of day and night closed-loop control by comparing the md-logic automated insulin delivery system to sensor augmented pump therapy in patients with type 1 diabetes at home. *Diabetes, Obesity and Metabolism*, 21(4):822–828, 2019.

[6] P. Colmegna, F. Bianchi, and R. Sánchez-Peña. Automatic glucose control during meals and exercise in type 1 diabetes: Proof-of-concept in silico tests using a switched LPV approach. *IEEE Control System Letters*, 5(5):1489–94, 2021.

[7] P. Colmegna, F. Garelli, H. De Battista, and R. Sánchez-Peña. Automatic regulatory control in type 1 diabetes without carbohydrate counting. *Control Engineering Practice*, 74:22–32, 2018.

[8] P. Colmegna, R. Sánchez-Peña, and R. Gondhalekar. Linear parameter-varying model to design control laws for an artificial pancreas. *Biomedical Signal Processing and Control*, 40:204–213, Feb 2018.

[9] T. Danne, R. Nimri, T. Battelino, R. M. Bergenstal, et al. International consensus on use of continuous glucose monitoring. *Diabetes Care*, 40(12):1631–1640, 2017.

[10] Gregory P Forlenza, Faye M Cameron, et al. Fully closed-loop multiple model probabilistic predictive controller artificial pancreas performance in adolescents and adults in a supervised hotel setting. *Diabetes technology & therapeutics*, 20(5):335–343, 2018.

[11] E. Fushimi, P. Colmegna, H. De Battista, F. Garelli, and R.S. Sánchez-Peña. Artificial Pancreas: evaluating the ARG algorithm without meal announcement. *Journal of Diabetes Science and Technology*, 13(6):1035–1043, 2019.

[12] F. Garelli, E. Fushimi, N. Rosales, et al. First outpatient clinical trial of a full closed-loop artificial pancreas system in South America. *Journal of Diabetes Science and Technology*, page in press, 2022.

[13] F. Garelli, N. Rosales, E. Fushimi, D. Arambarri, L. Mendoza, et al. Remote glucose monitoring platform for multiple simultaneous patients at coronavirus disease 2019 intensive care units: Case report including adults and children. *Diabetes Technology & Therapeutics*, 23(6):471–473, June 2021.

[14] Konstanze Kölle, Torben Biester, Sverre Christiansen, Anders Lyngvi Fougner, and Øyvind Stavdahl. Pattern recognition reveals characteristic postprandial glucose changes: Non-individualized meal detection in diabetes mellitus type 1. *IEEE journal of biomedical and health informatics*, 24(2):594–602, 2019.

[15] J. Löfberg. YALMIP: A toolbox for modeling and optimization in MATLAB. In *In Proc. CACSD Conf.*, Taipei, Taiwan, 2004.

[16] Zeinab M., D. Boiroux, F. Cameron, N. Kjølstad Poulsen, B. W. Bequette, and J. B. Jørgensen. An automated meal detector and bolus calculator in combination with closed-loop blood glucose control. *IFAC-PapersOnLine*, 51(27):168–173, 2018. 10th IFAC Symposium on Biological and Medical Systems BMS 2018.

[17] M. Moscoso-Vasquez, P. Colmegna, N. Rosales, F. Garelli, and R. Sánchez-Peña. Control-oriented model with intra-patient variations for an artificial pancreas. *IEEE Journal of Biomedical and Health Informatics*, 24(9):2681–2689, 2020.

[18] Emilie Palisaitis, Anas El Fathi, Julia E von Oettingen, Ahmad Haidar, and Laurent Legault. A meal detection algorithm for the artificial pancreas: a randomized controlled clinical trial in adolescents with type 1 diabetes. *Diabetes Care*, 44(2):604–606, 2021.

[19] Jordan E Pinsker, Eyal Dassau, Sunil Deshpande, Dan Raghinaru, Bruce A Buckingham, Yogish C Kudva, Lori MB Laffel, Carol Levy, Mei Mei Church, Hannah Desrochers, et al. Outpatient randomized crossover comparison of zone model predictive control automated insulin delivery with weekly data driven adaptation versus sensor-augmented pump: Results from the international diabetes closed loop trial 4 (dclp4). *Diabetes Technology and Therapeutics*, (ja), 2022.

[20] A. N. Pitsillides, S. M. Anderson, and B. Kovatchev. Hypoglycemia risk and glucose variability indices derived from routine self-monitoring of blood glucose are related to laboratory measures of insulin sensitivity and epinephrine counterregulation. *Diabetes Technology & Therapeutics*, 13(1):11–17, 2008.

[21] C. M. Ramkissoon, P. Herrero, J. Bondia, and J. Vehi. Unannounced meals in the artificial pancreas: Detection using continuous glucose monitoring. *Sensors*, 18(3), 2018.

[22] A. Revert, F. Garelli, J. Picó, H. De Battista, P. Rossetti, J. Vehi, and J. Bondia. Safety auxiliary feedback element for the artificial pancreas in type 1 diabetes. *IEEE Transactions on Biomedical Engineering*, 60(8):2113–2122, 2013.

[23] R. S. Sánchez-Peña, P. Colmegna, L. Grosembacher, et al. Artificial Pancreas: First clinical trials in Argentina. In *20th IFAC World Congress*, pages 7997–8002, Toulouse, France, 2017.

[24] R. S. Sánchez-Peña and D. R. Cherñavvsky. *The Artificial Pancreas: Current Situation and Future Directions*. Academic Press, 2019.

[25] R. Sanz, Pedro García, José-Luis Díez, and Jorge Bondia. Artificial pancreas system with unannounced meals based on a disturbance observer and feedforward compensation. *IEEE Transactions on Control Systems Technology*, 29(1):454–460, 2021.

[26] Paramesh Shamanna, Mala Dharmalingam, Rakesh Sahay, Jahangir Mohammed, Maluk Mohamed, Terrence Poon, Nathan Kleinman, and Mohamed Thajudeen. Retrospective study of glycemic variability, bmi, and blood pressure in diabetes patients in the digital twin precision treatment program. *Scientific Reports*, 11(1):1–9, 2021.

[27] Jos F Sturm. Using SeDuMi 1.02, a MATLAB toolbox for optimization over symmetric cones. *Optimization methods and software*, 11(1-4):625–653, 1999.

[28] Xiaoyu Sun, Mudassir Rashid, Nicole Hobbs, Rachel Brandt, Mohammad Reza Askari, and Ali Cinar. Incorporating prior information in adaptive model predictive control for multivariable artificial pancreas systems. *Journal of Diabetes Science and Technology*, 16(1):19–28, 2022.

[29] R. Sánchez-Peña, P. Colmegna, F. Garelli, H. De Battista, et al. Artificial pancreas: Clinical study in Latin America without premeal insulin boluses. *Journal of Diabetes Science and Technology*, 12(5):914–925, 2018.

[30] Akemi Tokutsu, Yosuke Okada, Keiichi Torimoto, and Yoshiya Tanaka. Relationship between interstitial glucose variability in ambulatory glucose profile and standardized continuous glucose monitoring metrics; a pilot study. *Diabetology & metabolic syndrome*, 12(1):1–7, 2020.

[31] Fei Zheng, Stéphane Bonnet, Emma Villeneuve, Maeva Doron, Aurore Lepecq, and Florence Forbes. Unannounced meal detection for artificial pancreas systems using extended isolation forest. In *2020 42nd Annual International Conference of the IEEE Engineering in Medicine & Biology Society (EMBC)*, pages 5892–5895, 2020.